

## Supplemental information for:

# An irreversible inhibitor to probe the role of *Streptococcus pyogenes* cysteine protease SpeB in evasion of host complement defenses

Jordan L. Woehl<sup>1#</sup>, Seiya Kitamura<sup>1#</sup>, Nicholas Dillon<sup>3</sup>, Zhen Han<sup>1</sup>, Landon J. Edgar<sup>1</sup>, Victor Nizet<sup>3,4</sup>, Dennis W. Wolan<sup>1,2\*</sup>

<sup>1</sup>Department of Molecular Medicine, <sup>2</sup>Department of Integrative Structural and Computational Biology, The Scripps Research Institute, La Jolla, CA 92037.

<sup>3</sup>Division of Host-Microbe Systems & Therapeutics, Department of Pediatrics, <sup>4</sup>Skaggs School of Pharmacy and Pharmaceutical Sciences, UC San Diego, La Jolla, CA, USA.

\*Corresponding author: [wolan@scripps.edu](mailto:wolan@scripps.edu).

#Equal contribution

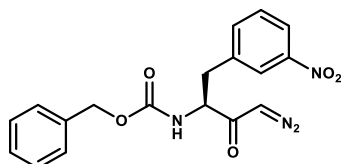
## Table of Contents

<b>S1</b>	Detailed synthetic methods and compound characterization.
<b>S4</b>	Table S1. X-ray data collection and structure refinement statistics of SpeB in complex with <b>2S</b> .
<b>S5</b>	Figure S1. Specificity of SpeB inhibitors.
<b>S6</b>	Figure S2. $K_i$ determination of compound <b>1S</b> .
<b>S7</b>	Figure S3. Reversibility of covalent SpeB inhibitors <b>2S-CMK</b> and <b>2S</b> .
<b>S8</b>	Figure S4. $k_{inact}$ and $K_i$ determination of <b>2S</b> .
<b>S9</b>	Figure S5. Electron density of <b>2S</b> bound to SpeB.
<b>S10</b>	Figure S6. Labeling of rSpeB and papain by <b>2S-alkyne</b> and in-gel fluorescence visualization.
<b>S11</b>	Figure S7. Compound <b>2S-alkyne</b> restores AP-mediated hemolysis of Er, raw values.
<b>S12</b>	Figure S8. Exogenously added SpeB inhibits complement-mediated C3b deposition on WT <i>S. pyogenes</i> cells in a dose-dependent manner.
<b>S13</b>	Figure S9. Toxicity of compounds on Jurkat T cells.
<b>S14</b>	Supporting Information References.

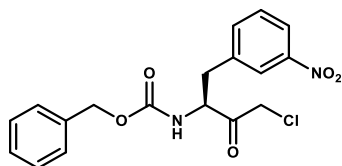
## Detailed synthetic methods and compound characterization

### General

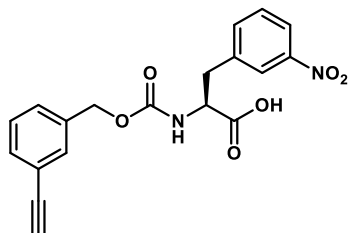
All reagents and solvents were purchased from commercial suppliers and were used without further purification.  $^1\text{H}$  and  $^{13}\text{C}$  NMR spectra were collected using a Bruker 600, 500, or 400 MHz spectrometer with chemical shifts reported relative to residual deuterated solvent peaks or a tetramethylsilane internal standard. Accurate masses were measured using an ESI-TOF (HRMS, Agilent MSD) or MSQ Plus mass spectrometer (LRMS, Thermo Scientific). Reactions were monitored on TLC plates (silica gel 60, F254 coating, EMD Millipore, 1057150001), and spots were either monitored under UV light (254 nm) or stained with phosphomolybdic acid. The same TLC system was used to test purity, and all final products showed a single spot on TLC with both  $\text{KMnO}_4$  and UV absorbance. The purity of the compounds that were tested in the assay was >95% based on  $^1\text{H}$  NMR and reverse phase HPLC-UV on monitoring absorption at 240 nm. It should be noted that SpeB is susceptible to divalent cations such as  $\text{Cu}^{2+}$ ,  $\text{Zn}^{2+}$ ; thus, care was taken to ensure that the final products did not contain contaminations of these metals.



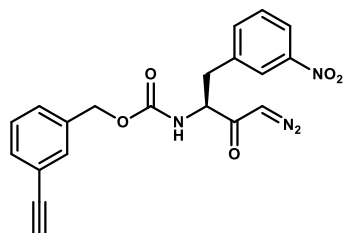
(S)-2-(((benzyloxy)carbonyl)amino)-3-(3-nitrophenyl)propanoic acid was synthesized previously.<sup>1</sup> Carboxylic acid was converted into diazoketone using a method previously described. To a stirred solution of (S)-2-(((benzyloxy)carbonyl)amino)-3-(3-nitrophenyl)propanoic acid (500 mg, 1.45 mmol) in DCM at 0 °C was added dropwise N-methylmorpholine (154 mg, 1.53 mmol, 1.05 eq.) and isobutyl chloroformate (200  $\mu\text{L}$ , 1.53 mmol, 1.05 eq.). After 15 min, ethereal diazomethane was generated from Diazald® (931 mg, 4.35 mmol) in accordance to procedures outlined in Aldrich Technical Bulletin AL-180 and distilled into stirred solution over the course of 30 minutes. After distillation, the reaction was allowed to warm to r.t. and continue for 1 hour. Glacial acetic acid was added dropwise after being chilled to quench excess diazomethane. One third of the reaction was separated and the solvent was removed in vacuo, dissolved in ethyl acetate and subsequently washed with water, sat. aq.  $\text{NaHCO}_3$  twice, sat. aq.  $\text{NaCl}$ , dried over  $\text{MgSO}_4$ , and concentrated in vacuo. Recrystallization from acetone yielded the desired product as a white solid (45 mg, 0.12 mmol, 25%).  $^1\text{H}$  NMR (600 MHz,  $\text{DMSO}-d_6$ )  $\delta$  8.22 (t,  $J$  = 2.0 Hz, 1H), 8.10 (dd,  $J$  = 8.0, 2.4 Hz, 1H), 7.87 (d,  $J$  = 8.8 Hz, 1H), 7.76 (d,  $J$  = 7.6 Hz, 1H), 7.58 (t,  $J$  = 7.9 Hz, 1H), 7.34 – 7.26 (m, 3H), 7.21 – 7.16 (m, 2H), 6.28 (broad s, 1H), 4.96 (d,  $J$  = 12.7 Hz, 1H), 4.92 (d,  $J$  = 12.7 Hz, 1H), 4.38 – 4.32 (m, 1H), 3.20 (dd,  $J$  = 13.8, 4.2 Hz, 1H), 2.85 (dd,  $J$  = 13.8, 11.1 Hz, 1H).  $^{13}\text{C}$  NMR (151 MHz, DMSO)  $\delta$  193.9, 155.9, 147.6, 140.2, 136.8, 136.3, 129.6, 128.3, 127.8, 127.4, 124.0, 121.5, 65.4, 59.3, 53.4, 35.7. HRMS (+) calcd for  $(\text{M}+\text{Na})^+$  391.1013. Found 391.1018. Purity (HPLC-UV): 98%.



Two third of the reaction above was separated and to this mixture was added concn. aq.  $\text{HCl}$ . dropwise until the conversion completed. The solvent was removed in vacuo, dissolved in ethyl acetate and subsequently washed with water, sat. aq.  $\text{NaHCO}_3$  twice, sat. aq.  $\text{NaCl}$ , dried over  $\text{MgSO}_4$ , and concentrated in vacuo. Recrystallization from acetone yielded the desired product as White solid (160 mg, 0.43 mmol, 44%).  $^1\text{H}$  NMR (600 MHz,  $\text{DMSO}-d_6$ )  $\delta$  8.20 (t,  $J$  = 2.0 Hz, 1H), 8.10 (ddd,  $J$  = 8.2, 2.4, 1.0 Hz, 1H), 7.89 (d,  $J$  = 8.4 Hz, 1H), 7.73 (dt,  $J$  = 7.6, 1.4 Hz, 1H), 7.58 (t,  $J$  = 7.9 Hz, 1H), 7.35 – 7.26 (m, 3H), 7.23 – 7.18 (m, 2H), 4.99 – 4.90 (m, 2H), 4.76 (d,  $J$  = 16.9 Hz, 1H), 4.71 (d,  $J$  = 16.9 Hz, 1H), 4.56 (ddd,  $J$  = 10.8, 8.4, 4.1 Hz, 1H), 3.30 (dd,  $J$  = 13.8, 4.1 Hz, 1H), 2.85 (dd,  $J$  = 13.9, 10.8 Hz, 1H).  $^{13}\text{C}$  NMR (151 MHz, DMSO)  $\delta$  200.3, 156.0, 147.6, 140.0, 136.7, 136.3, 129.6, 128.3, 127.8, 127.5, 124.0, 121.6, 65.6, 59.1, 47.7, 34.4. HRMS (+) calcd for  $(\text{M}+\text{H})^+$  377.0899. Found 377.0909. Purity (HPLC-UV): >99%.



(3-ethynylphenyl)methanol was synthesized using the method described previously.<sup>2, 3</sup> Spectral data matched with reported values.<sup>2</sup> Target carbamate was synthesized from the (3-ethynylphenyl)methanol and (S)-2-amino-3-(3-nitrophenyl)propanoic acid using the method<sup>1</sup> described previously (1.26 g (3.42 mmol, 94%). <sup>1</sup>H NMR (600 MHz, Chloroform-*d*)  $\delta$  8.10 (s, 1H), 7.54 – 7.39 (m, 5H), 7.31 (d, *J* = 6.8 Hz, 3H), 5.37 (d, *J* = 7.8 Hz, 1H), 5.09 – 5.01 (m, 2H), 4.75-4.70 (m, 1H), 3.36 (dd, *J* = 14.0, 5.5 Hz, 1H), 3.19 (dd, *J* = 14.2, 6.4 Hz, 1H), 3.09-3.07 (m, 1H), 3.02 – 2.96 (m, 1H). <sup>13</sup>C NMR (151 MHz, Chloroform-*d*)  $\delta$  173.50, 155.07, 147.81, 137.42, 135.86, 135.23, 131.49, 131.12, 129.09, 129.04, 126.91, 123.81, 121.99, 121.87, 82.73, 77.16, 66.08, 53.92, 30.48. LRMS (+) calcd for (M+H)<sup>+</sup> 369.1. Found 369.2.



Target molecule was synthesized using the method described for benzyl (S)-(4-diazo-1-(3-nitrophenyl)-3-oxobutan-2-yl)carbamate (300 mg (0.76 mmol, 50%)). <sup>1</sup>H NMR (600 MHz, DMSO-*d*<sub>6</sub>)  $\delta$  8.22 (s, 1H), 8.09 (d, *J* = 8.4 Hz, 1H), 7.91 (d, *J* = 8.9 Hz, 1H), 7.76 (d, *J* = 7.8 Hz, 1H), 7.57 (t, *J* = 7.9 Hz, 1H), 7.42 – 7.26 (m, 4H), 7.24 (d, *J* = 7.8 Hz, 1H), 6.29 (s, 1H), 4.95 (s, 2H), 4.34 (s, 1H), 4.19 (d, *J* = 7.0 Hz, 2H), 3.20 (dd, *J* = 13.9, 4.2 Hz, 1H), 2.86 (dd, *J* = 13.8, 11.1 Hz, 1H). <sup>13</sup>C NMR (151 MHz, DMSO)  $\delta$  193.8, 155.8, 147.6, 140.2, 137.5, 136.2, 131.0, 130.5, 129.5, 128.7, 127.9, 124.0, 121.7, 121.5, 83.1, 80.9, 64.8, 59.3, 53.4, 35.7. HRMS (+) calcd for (M+Na)<sup>+</sup> 415.1013. Found 415.1018. Purity (HPLC-UV): 96%.

**Table S1.** X-ray crystallography data collection and refinement statistics.

PDB ID	6UKD
Wavelength (Å)	0.97946
Space group	P2 <sub>1</sub> 2 <sub>1</sub>
Unit Cell Parameters (a,b,c) (Å)	37.27,50.40,114.50
Data Processing	
Resolution range (Å) (outer shell)	37.27-1.58 (1.66-1.59)
Unique reflections	29,409 (2,644)
Completeness (%)	98.3 (90.0)
Redundancy	5.8 (3.5)
R <sub>meas</sub> (%) <sup>a</sup>	11.5 (47.7)
R <sub>merge</sub> (%) <sup>b</sup>	8.7 (40.4)
R <sub>p.i.m.</sub> (%) <sup>c</sup>	4.5 (22.2)
Average I/σ(I)	17.4 (2.2)
Wilson B (Å <sup>2</sup> )	14.0
Refinement	
Resolution range (Å)	37.27-1.59 (1.65-1.59)
No. reflections (test set) <sup>d</sup>	29,406 (1,048)
R <sub>cryst</sub> (%) <sup>e</sup>	15.3 (20.7)
R <sub>free</sub> (%)	18.9 (25.7)
Protein atoms / waters / ligands	2,000 / 317 / 33
CV coordinate error (Å) <sup>f</sup>	0.15
Rmsd bonds (Å) / angles (°)	0.009 / 1.01
B-values protein/waters/ligands (Å <sup>2</sup> )	13.4 / 27.4 / 25.2
Ramachandran Statistics (%)	
Most favored	98.4
Additional allowed	1.6
Generously allowed	0.0

<sup>a</sup> $R_{\text{meas}} = \frac{1}{\sum_{hkl} \sum_i I_{i(hkl)}}$ , where  $I_{i(hkl)}$  are the observed intensities,  $\langle I_{(hkl)} \rangle$  are the average intensities and  $N$  is the multiplicity of reflection  $hkl$ . <sup>b</sup> $R_{\text{merge}} = \frac{\sum_{hkl} \sum_i |I_{i(hkl)} - \langle I_{(hkl)} \rangle|}{\sum_{hkl} \sum_i I_{i(hkl)}}$  where  $I_{i(hkl)}$  is the  $i^{\text{th}}$  measurement of reflection  $h$  and  $\langle I_{(hkl)} \rangle$  is the average measurement value. <sup>c</sup> $R_{\text{p.i.m.}}$  (precision-indicating  $R_{\text{merge}}$ ) =  $\sum_{hkl} [1/(N_{hkl} - 1)]^{1/2} \sum_i |I_{i(hkl)} - \langle I_{(hkl)} \rangle| / \sum_{hkl} \sum_i I_{i(hkl)}$ . <sup>d</sup>Reflections with  $I > 0$  were used for refinement. <sup>e</sup> $R_{\text{cryst}} = \sum_h ||F_{\text{obs}}| - |F_{\text{calc}}|| / \sum |F_{\text{obs}}|$ , where  $F_{\text{obs}}$  and  $F_{\text{calc}}$  are the calculated and observed structure factor amplitudes, respectively.  $R_{\text{free}}$  is  $R_{\text{cryst}}$  with 5.0% test set structure factors. <sup>f</sup>Cross-validated (CV) Luzzati coordinate errors.

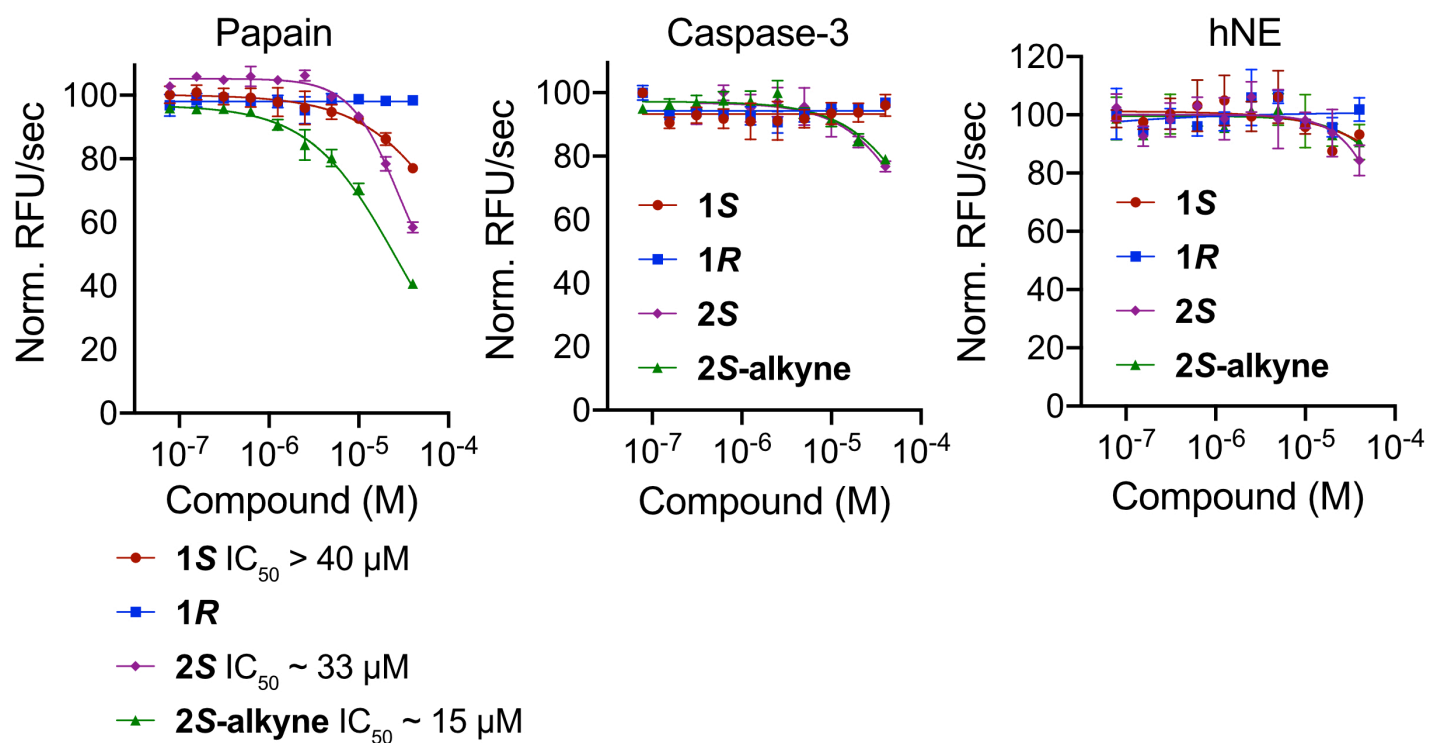


**Figure S1.** Specificity of SpeB inhibitors. Dose-response curves of each compound against papain (Ac-AIK-AMC), caspase-3 (Ac-DEVD-AMAC), or hNE (Ac-AAPV-AMC). Each compound was assessed over a 2-fold logarithmic dilution series.  $IC_{50}$  values were measured based on 10-min incubation and are shown in mean  $\pm$  SD ( $n \geq 3$ ).

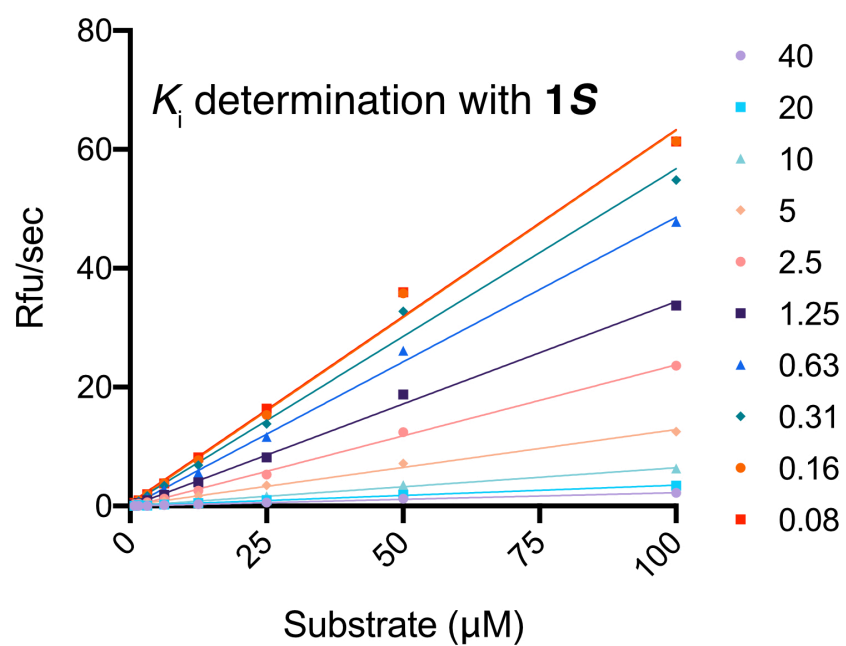


**Figure S2.**  $K_i$  determination of compound **1S**. Dose-response curves of **1S** against rSpeB with changes in substrate (Ac-AIK-AMC) concentration are shown.

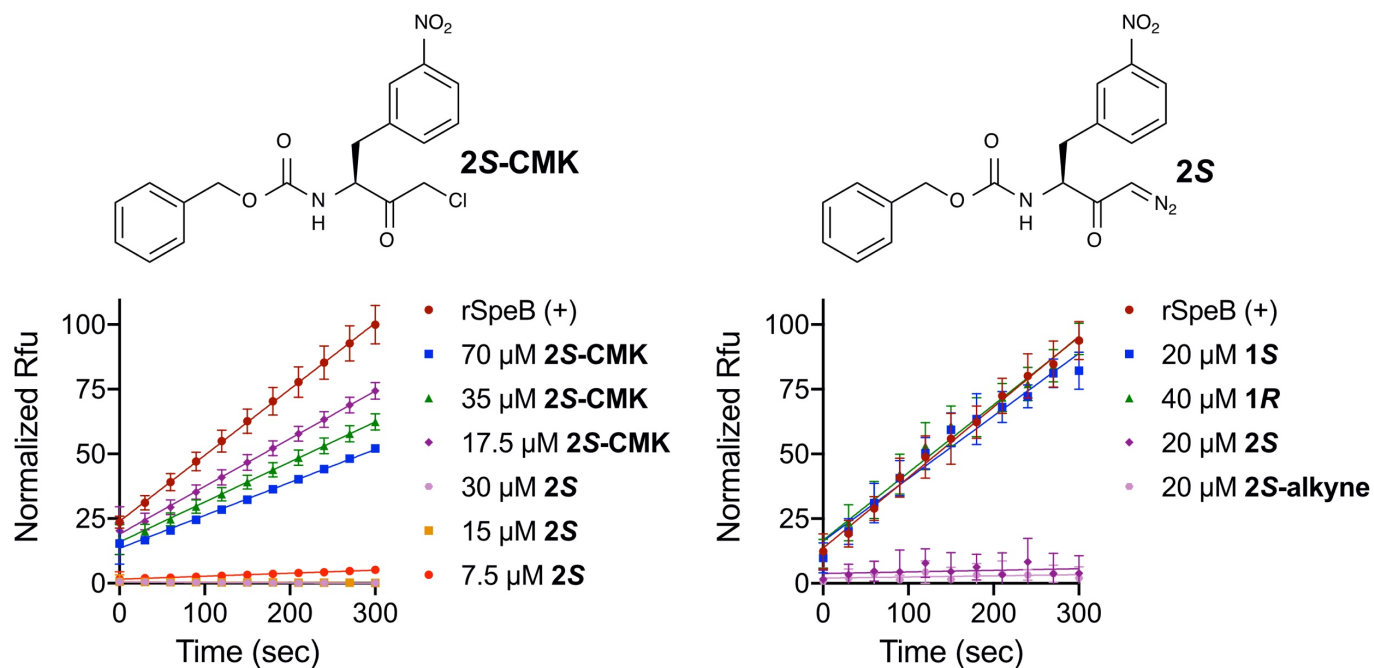


**Figure S3.** Reversibility of SpeB inhibitors. Compounds **2S-CMK** ( $IC_{50} = \sim 6.7 \mu M$ ) and **2S** ( $IC_{50} = \sim 1.9 \mu M$ ) incubated for 30 min at a concentration  $\sim 10$ -fold above the  $IC_{50}$  with rSpeB ( $2 \mu M$ ) at 100-fold the activity assay concentration. Following incubation, reaction mixture diluted 1:100 in assay buffer and substrate added. Loss of SpeB inhibition over time is shown with **2S-CMK**, but not with **2S**, suggesting **2S** is an irreversible inhibitor. Similar assay run with compounds **1S**, **1R**, **2S**, and **2S-alkyne** shows **2S/2S-alkyne** are the only irreversible inhibitors.

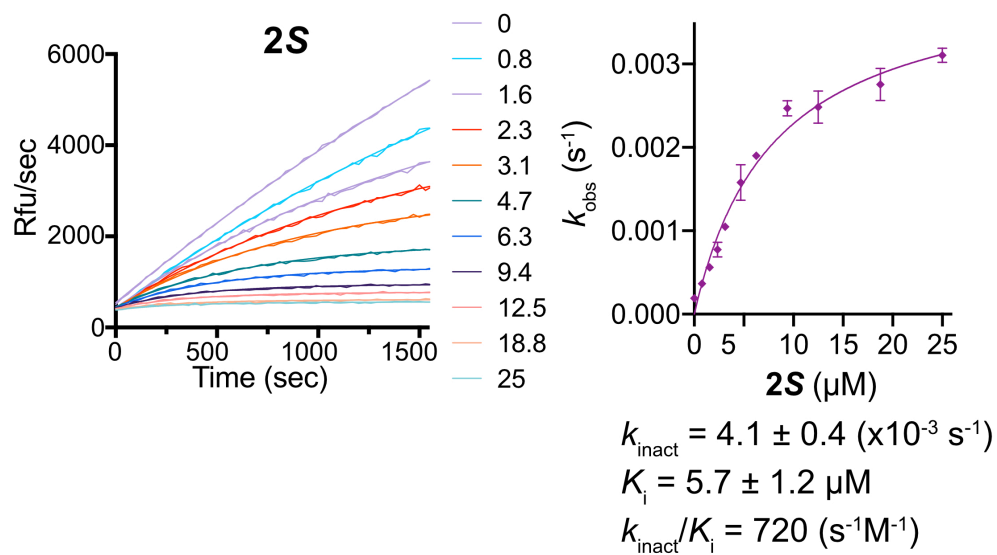


**Figure S4.**  $k_{\text{inact}}$  and  $K_i$  determination of **2S**. Dose-response curves of each compound against rSpeB with a constant substrate (Ac-AIK-AMC) concentration of 100  $\mu\text{M}$ .  $K_i$  and  $k_{\text{inact}}$  values were determined using the model described by Kuzmič *et al.*<sup>5</sup>



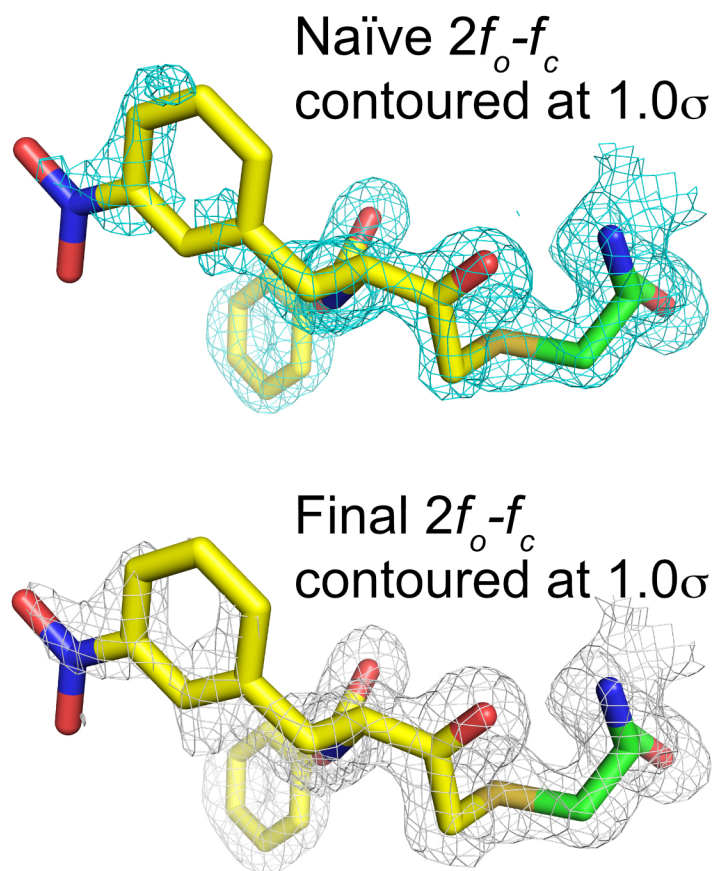


**Figure S5.** Electron density of **2S** bound to SpeB. Naïve  $2f_o-f_c$  map contoured at  $1.0\sigma$  and final  $2f_o-f_c$  map contoured at  $1.0\sigma$  clearly delineates the binding of **2S** to C192 and orientation of the compound in the active site of SpeB. Residues of Cys192 (green) and **2S** shown as a stick model with yellow carbon, red oxygen, blue nitrogen, and mustard sulfur.

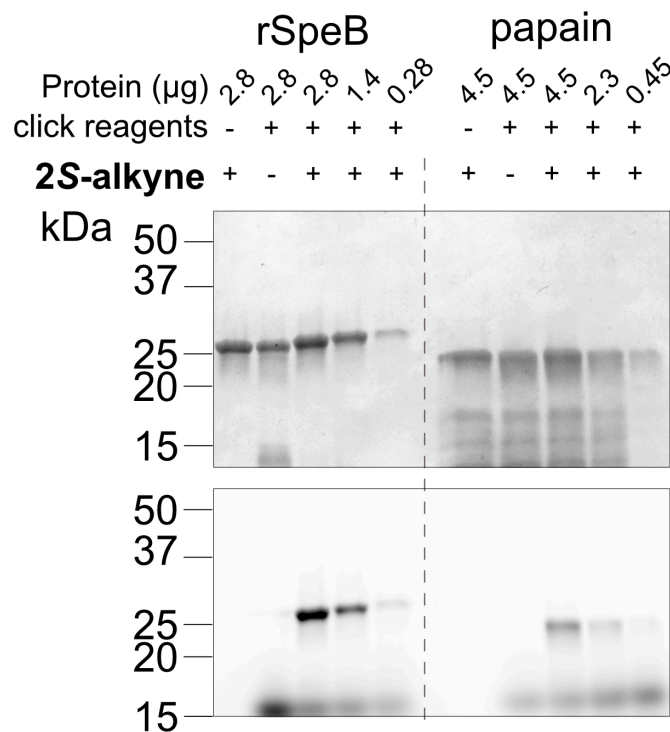


**Figure S6.** *In situ* labeling of rSpeB and papain with **2S-alkyne**. Recombinant SpeB (2.8 to 0.28 μg) and papain (4.5 to 0.45 μg) were labeled with **2S-alkyne** with Coomassie stain (top) and in-gel fluorescence (bottom). Recombinant SpeB and papain were incubated in 40 μL with 100 μM **2S-alkyne** or DMSO (control) at 25 °C for 30 min. Click cocktail was added into the protein-probe mixture with final concentrations of 100 μM CuSO<sub>4</sub>, 500 μM BTAA (Click Chemistry Tools), 5 mM sodium ascorbate, and 100 μM AFDye 647 Azide (Click Chemistry Tools). The reaction mixtures were incubated at 25 °C for 1 h. 10 μL was removed and combined with 3.3 μL SDS-PAGE loading dye. Samples were resolved on a 4-20% SDS-PAGE gradient gel, destained, and imaged using a Chemidoc MP Imaging System (Bio-Rad).

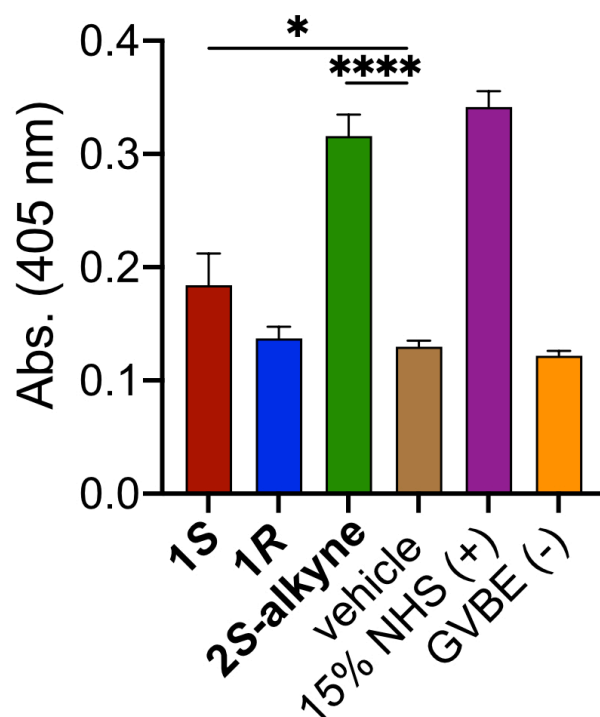


**Figure S7.** Compound **2S-alkyne** restores AP-mediated hemolysis of Er, raw values. The ability of the compounds to restore AP-mediated hemolysis of Er was assessed using a fixed concentration of rSpeB (5  $\mu$ M), NHS [15% (v/v)], and compound (20  $\mu$ M). Values represent absorbance (Abs.) at 405 nm with no normalization to controls. 15% (v/v) NHS alone represents the positive control; GHBS<sup>o</sup> + EDTA (GVBE) represents the negative control from the ability of EDTA to knockout alternative pathway metal-dependent activation. Data are shown as mean  $\pm$  SD ( $n \geq 3$ ). \* $p$ -value = 0.024, \*\*\*\* =  $<0.0001$  using a one-way ANOVA test.

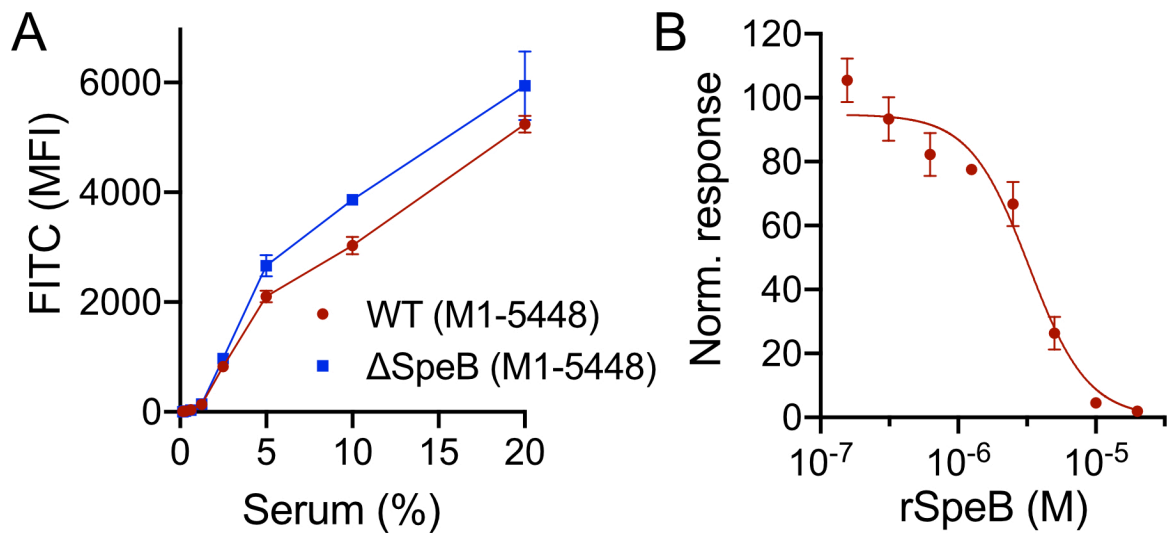


**Figure S8.** Exogenously added SpeB inhibits complement-mediated C3b deposition on WT and  $\Delta$ speB *S. pyogenes* cells in a dose-dependent manner. *S. pyogenes* was grown overnight, diluted in assay buffer, and incubated with NHS in a dose-dependent manner [0.2 to 25% (v/v)] and C3b deposition was analyzed using a FITC-conjugated anti-C3b antibody. (A) C3b deposition is increased in correlation to NHS (%). (B) At a single percentage of NHS (10%), exogenous SpeB was added in a dose-dependent manner to NHS/WT bacteria and C3b deposition was analyzed. Inhibition of C3b deposition by SpeB was normalized to 10% NHS (100% MFI) and 0% NHS (0% MFI) controls. Values are represented as MFI and are shown as mean  $\pm$  SD ( $n \geq 3$ ).

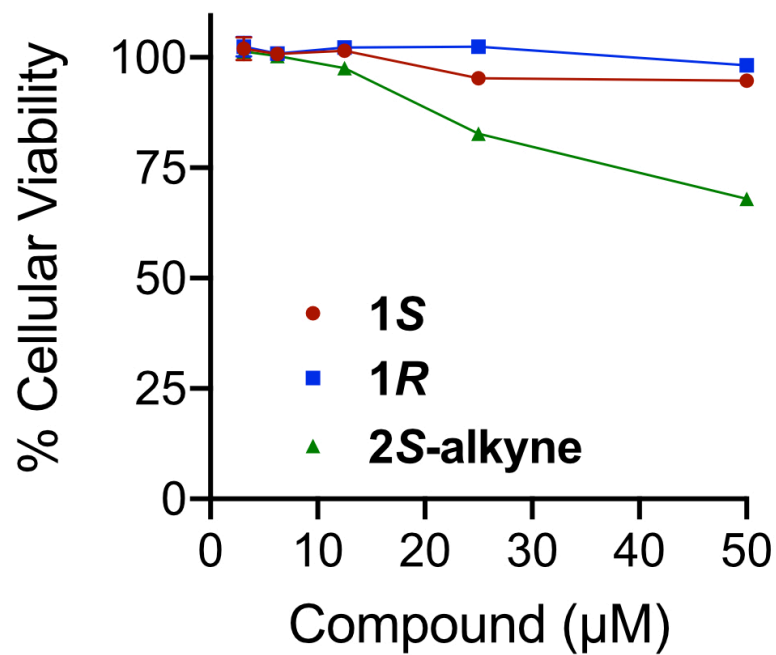


**Figure S9.** Toxicity of compounds on Jurkat T cells. Cells were treated with increasing concentrations of SpeB inhibitors or DMSO vehicle for 3 h and cellular viability was measured using CellTiter-Glo®. Each data point is shown as mean  $\pm$  SD ( $n \geq 3$ ).

## Supplementary information references

1. Kitamura, S.; Zheng, Q.; Woehl, J. L.; Solania, A.; Chen, E.; Dillon, N.; Hull, M.; Kotaniguchi, M.; Kitamura, S.; Nizet, V.; Sharpless, K. B.; Wolan, D. W., SuFEx-enabled high-throughput medicinal chemistry. *J. Am. Chem. Soc.* **2020**, online. doi: 10.1021/jacs.9b13652.
2. Zhang, Q.; Takacs, J. M., Click-connected ligand scaffolds: macrocyclic chelates for asymmetric hydrogenation. *Org. Lett.* **2008**, *10* (4), 545-8.
3. Kitamura, S.; Hvorecny, K. L.; Niu, J.; Hammock, B. D.; Madden, D. R.; Morisseau, C., Rational design of potent and selective inhibitors of an epoxide hydrolase virulence factor from *Pseudomonas aeruginosa*. *J. Med. Chem.* **2016**, *59* (10), 4790-9.
4. Emsley, P.; Lohkamp, B.; Scott, W. G.; Cowtan, K., Features and development of Coot. *Acta Crystallogr. D* **2010**, *66*, 486-501.
5. Kuzmič, P.; Solowiej, J.; Murray, B. W., An algebraic model for the kinetics of covalent enzyme inhibition at low substrate concentrations. *Anal. Biochem.* **2015**, *484*, 82-90.